Loading-Dependent Elemental Composition of α-pinene SOA Particles

Citation	Schilling, John E., Qi Chen, Stephanie M. King, Thomas Rosenoern, Jesse H. Kroll, Douglas R. Worsnop, Peter F. DeCarlo, Allison C. Aiken, Donna Sueper, Jose L. Jimenez, and Scot T. Martin. 2009. “Loading-Dependent Elemental Composition of α-Pinene SOA Particles.” Atmospheric Chemistry and Physics 9 (3) (February 2): 771–782.
Published Version	http://www.atmos-chem-phys.net/9/771/2009/
Accessed	February 17, 2015 6:54:30 PM EST
Citable Link	http://nrs.harvard.edu/urn-3:HUL.InstRepos:12211483
Terms of Use	This article was downloaded from Harvard University's DASH repository, and is made available under the terms and conditions applicable to Open Access Policy Articles, as set forth at http://nrs.harvard.edu/urn-3:HUL.InstRepos:dash.current.terms-of-use#OAP

(Article begins on next page)

Supplementary Material For: Loading-Dependent Elemental Composition of α-Pinene SOA Particles

by

John E. Shilling,[1,†] Qi Chen,[1] Stephanie M. King,[1] Thomas Rosenoern,[1] Jesse H. Kroll,[2] Douglas R. Worsnop,[2] Peter F. DeCarlo,[3,4,‡] Allison C. Aiken,[4,5] Donna Sueper,[2,4,5] Jose L. Jimenez,[4,5] and Scot T. Martin[1,6*]

[1] School of Engineering and Applied Sciences, Harvard University, Cambridge, MA 02138

[2] Aerodyne Research, Inc., Billerica, MA 08121

[3]Department of Atmospheric and Oceanic Sciences University of Colorado, Boulder, CO 80309

[4]Cooperative Institute for Research in the Environmental Sciences (CIRES), University of Colorado, Boulder, CO 80309

[5]Department of Chemistry and Biochemistry, University of Colorado, Boulder, CO 80309

[6]Department of Earth and Planetary Sciences, Harvard University, Cambridge, MA 02138

[†]Now at Pacific Northwest National Laboratory, Atmospheric Sciences and Global Change Division, Richland, WA 99352

[‡]Now at the Paul Scherrer Institut, Laboratory of Atmospheric Chemistry, Villigen-PSI, CH-5232

E-mail: scot_martin@harvard.edu

http://www.seas.harvard.edu/environmental-chemistry

*To Whom Correspondence Should be Addressed

Literature Cited

DeCarlo, P. F., Kimmel, J. R., Trimborn, A., Jayne, J. T., Aiken, A. C., Gonin, M., Fuhrer, K., Horvath, T., Docherty, K. S., Worsnop, D. R. and Jimenez, J. L.: A field-deployable high-resolution time-of-flight aerosol mass spectrometer, Anal. Chem., 78, 8281-8289, 2006.

Aiken, A. C., DeCarlo, P. F., Kroll, J. H., Worsnop, D. R., Huffman, J. A., Cocherty, K., Ulbrich, I. M., Mohr, C., Kimmel, J. R., Sueper, D., Zhang, Q., Sun, Y., Trimborn, A., Northway, M., Ziemann, P. J., Canagaratna, M. R., Alfarra, R., Prevot, A. S. H., Dommen, J., Duplissy, J., Metzger, A., Baltensperger, U. and Jimenez, J. L.: O/C and OM/OC ratios of primary, secondary, and ambient organic aerosols with high resolution time-of-flight aerosol mass spectrometry, Environ. Sci. Technol., 42, 4478-4485, 2008.

Docherty, K. S., Stone, E. A., Ulbrich, I. M., DeCarlo, P. F., Snyder, D. C., Schauer, J. J., Peltier, R. E., Weber, R. J., Murphy, S. N., Seinfeld, J. H., Grover, B. D., Eatough, D. J. and Jiimenez, J. L.: Apportionment of primary and secondary organic aerosols in southern California during the 2005 study of organic aerosols in Riverside (SOAR-1), Environ. Sci. Technol., 42, 7655-7662, 2008.

Schneider, J., Weimer, S., Drewnick, F., Borrmann, S., Helas, G., Gwaze, P., Schmid, O., Andreae, M. O. and Kirchner, U.: Mass spectrometric analysis and aerodynamic properties of various types of combustion-related aerosol particles, Int. J. Mass Spectrom., 258, 37-49, 2006.

Table S1. SOA particle mass loadings and the measured O/C and H/C atomic ratios used in the basis-set fitting (i.e., entries of Table 2).

Figure S1. Correlation plots between unit-mass-resolution signal intensity and high-resolution oxygen-to-carbon atomic ratio. Except for the bottom-left panel, vertical axes show the percent contribution of the signal intensity of the indicated *m*/*z* value to the total organic signal. For the bottom-left panel, the vertical axis shows the ratio of the signal intensity at *m*/*z* 44 to that at *m*/*z* 43.

Figure S2. Measured oxygen-to-carbon atomic ratio vs. the 44/org signal for SOA particles produced from the dark ozonolysis of α-pinene. The linear regression through the data is shown in the solid line. The data points and the regression of *Aiken et al.* (2008) for ambient ground and aircraft measurements during the MILAGRO campaign are also shown. Equations for the linear fits and correlation coefficients are given in the figure.

Figure S3. Example of the deconvolution of a high-resolution mass spectrum for fragments at *m*/*z* 43. Peaks representing high-resolution model fits of $C_2H_3O^+$ and $C_3H_7^+$ are shown in the figure (DeCarlo *et al*., 2006). Panel i shows the residual between the recorded data and model fits for panel ii (gold), panel iii (grey), and panel iv (red). Panel ii, which was recorded with the AMS chopper open, shows the mass spectrum of the particles and the background. Panel iii, which was recorded with the AMS chopper closed, shows the mass spectrum of the background. Panel iv, which shows the difference of panel iii from panel ii, represents the mass spectrum of the particles. In each panel, the open circles show the recorded signal (Hz). The solid lines show the model fits in gold, grey, or red for individual peaks and in black for the sum of the model fits. The solid green bars indicate the peak intensity of each fit.

Figure S4. Contribution of the signal intensity at *m/z* 60 to the total organic signal intensity (i.e., 60/org) for increasing SOA particle mass loading for the dark ozonolysis of α-pinene. The average 60/org across all loading is 0.23%. Increased signal at *m/z* 60 is interpreted as a marker of biomass burning particles when observed in the mass spectra of atmospheric particles (Schneider *et al.*, 2006; Docherty *et al.*, 2008). Figure S4, however, shows that some of the signal intensity at *m/z* 60 can also be attributed to SOA particles.

SOA loading (μg/m^3)	O/C	H/C
0.5	0.45	1.38
1.3	0.43	1.35
6.6	0.36	1.40
15.4	0.38	1.44
36.6	0.33	1.47
95.2	0.32	1.51
138.0	0.29	1.51

Table S1

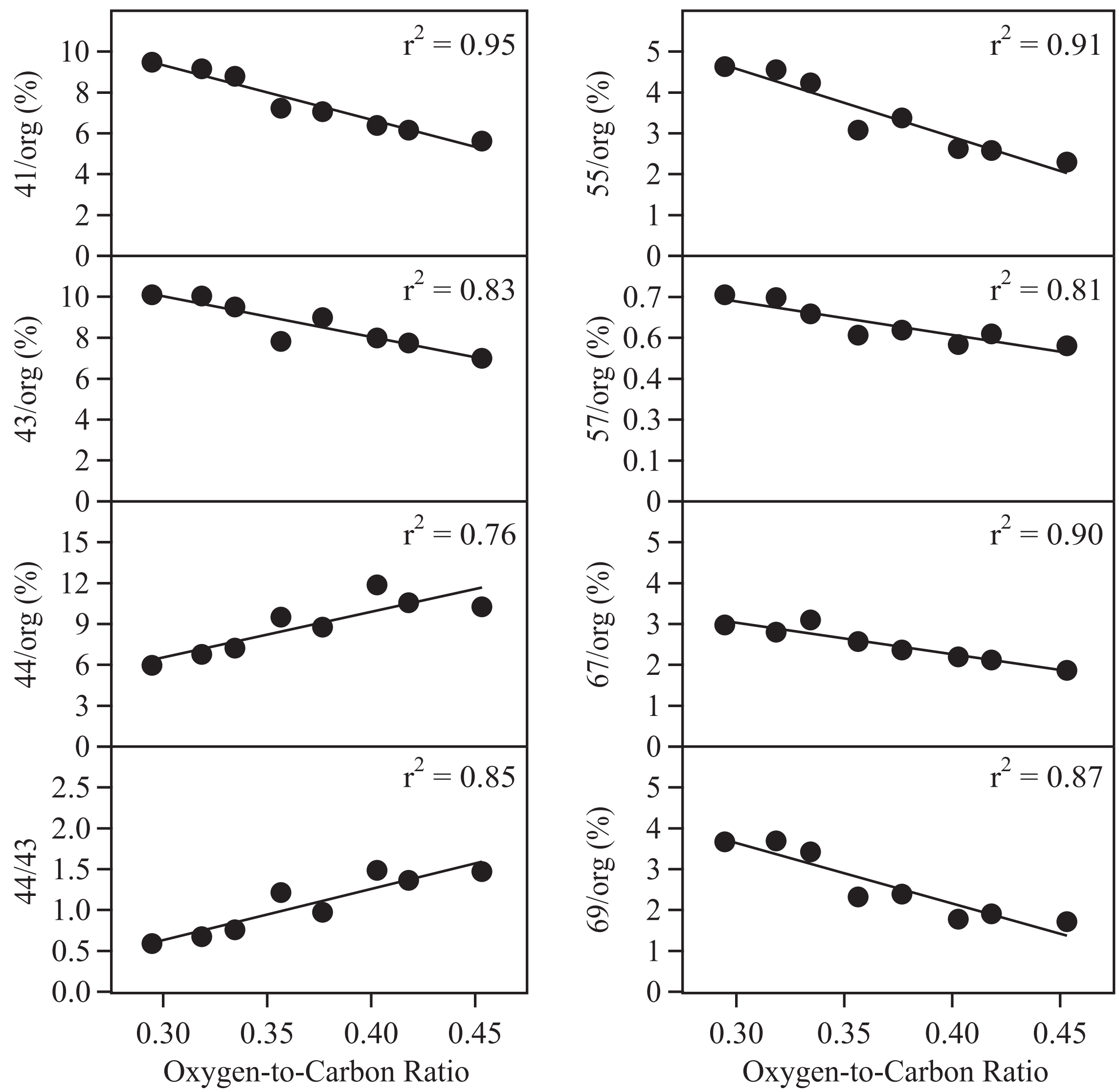

41/org (%)
43/org (%)
44/org (%)
44/43
55/org (%)
57/org (%)
67/org (%)
69/org (%)
r2 = 0.95
r2 = 0.83
r2 = 0.76
r2 = 0.85
r2 = 0.91
r2 = 0.81
r2 = 0.90
r2 = 0.87
0.30 0.35 0.40 0.45
Oxygen-to-Carbon Ratio
Oxygen-to-Carbon Ratio

Figure S1

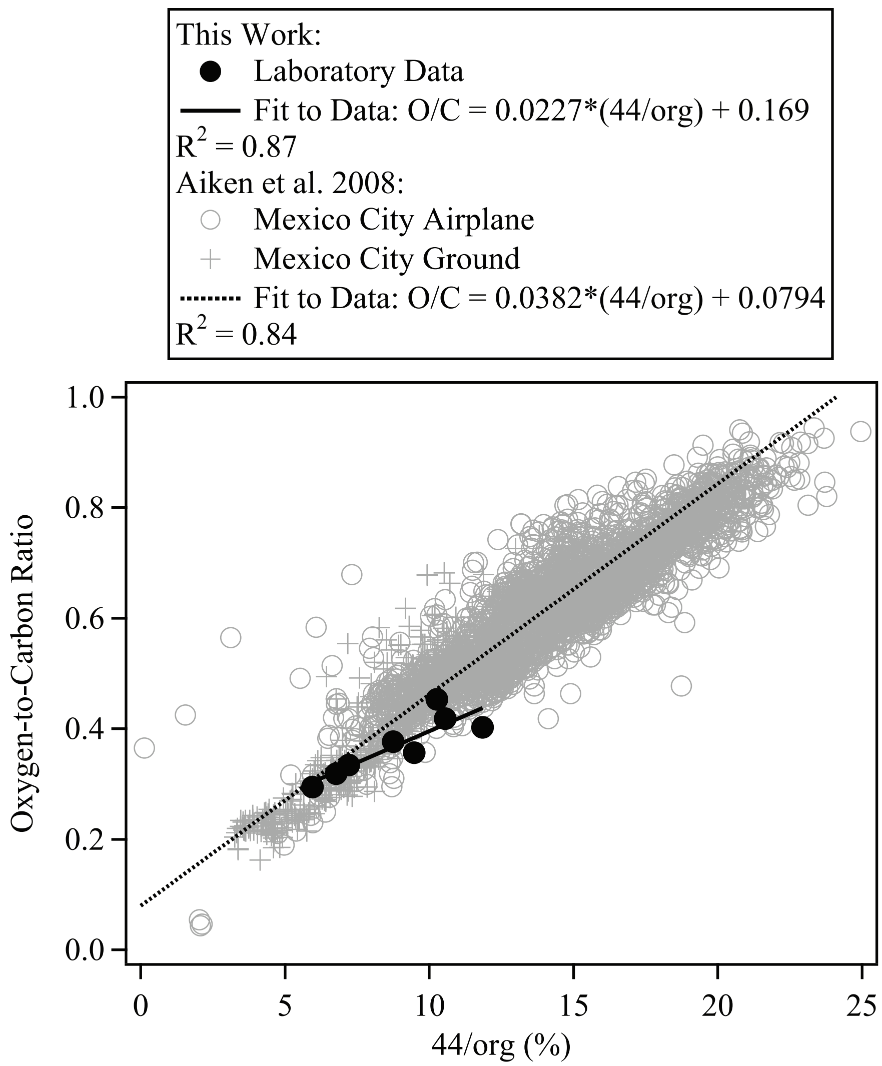
This Work:
Laboratory Data
Fit to Data: O/C = 0.0227*(44/org) + 0.169
R2 = 0.87
Aiken et al. 2008:
Mexico City Airplane
Mexico City Ground
Fit to Data: O/C = 0.0382*(44/org) + 0.0794
R2 = 0.84
1.0
0.8
0.6
0.4
0.2
0.0
Oxygen-to-Carbon Ratio
0
5
10
15
20
25
44/org (%)

Figure S2

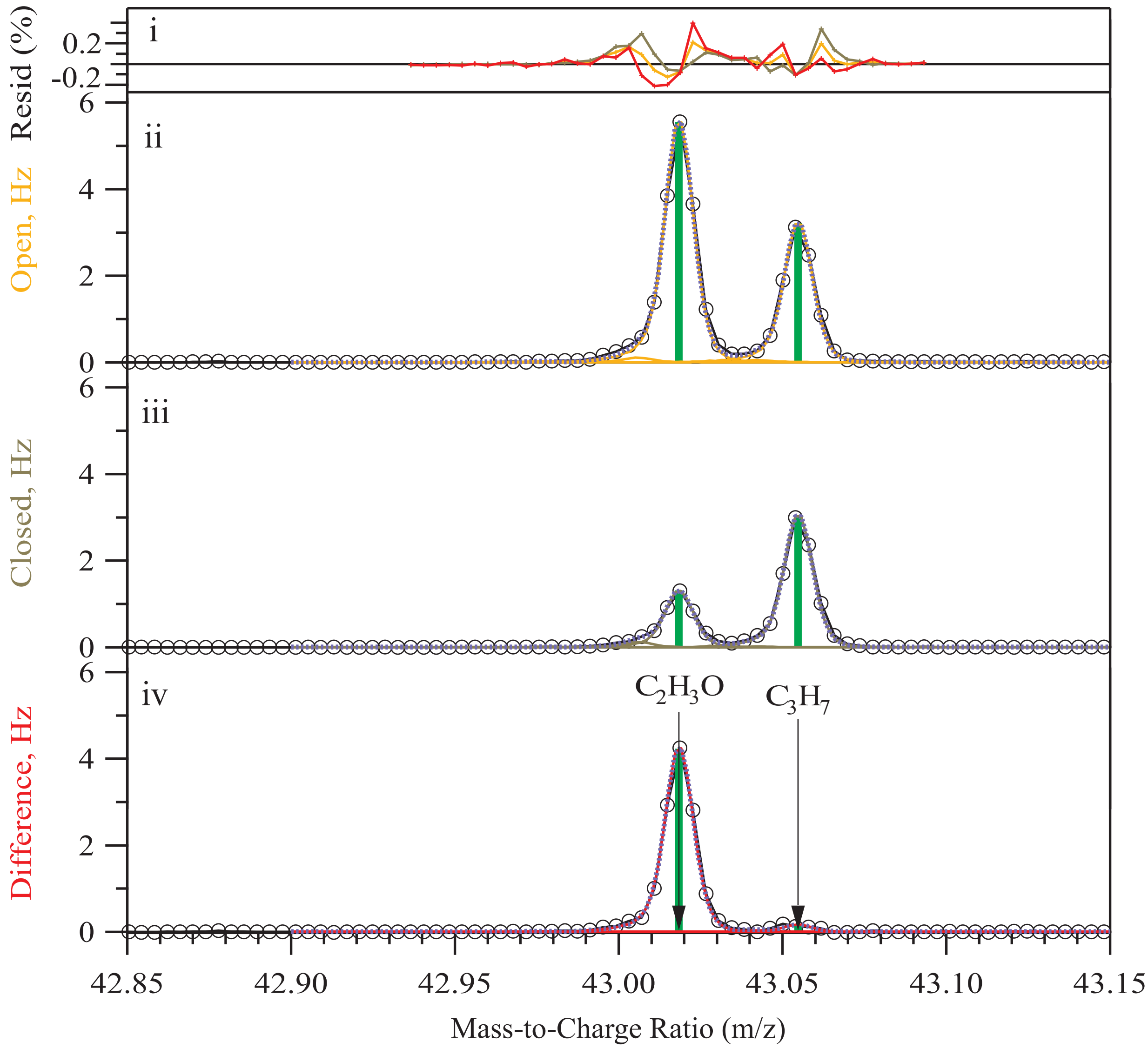

Resid (%)
0.2
-0.2
i
Open, Hz
6
4
2
0
ii
Closed, Hz
6
4
2
0
iii
Difference, Hz
6
4
2
0
iv
C_2H_3O
C_3H_7
42.85
42.90
42.95
43.00
43.05
43.10
43.15
Mass-to-Charge Ratio (m/z)

Figure S3

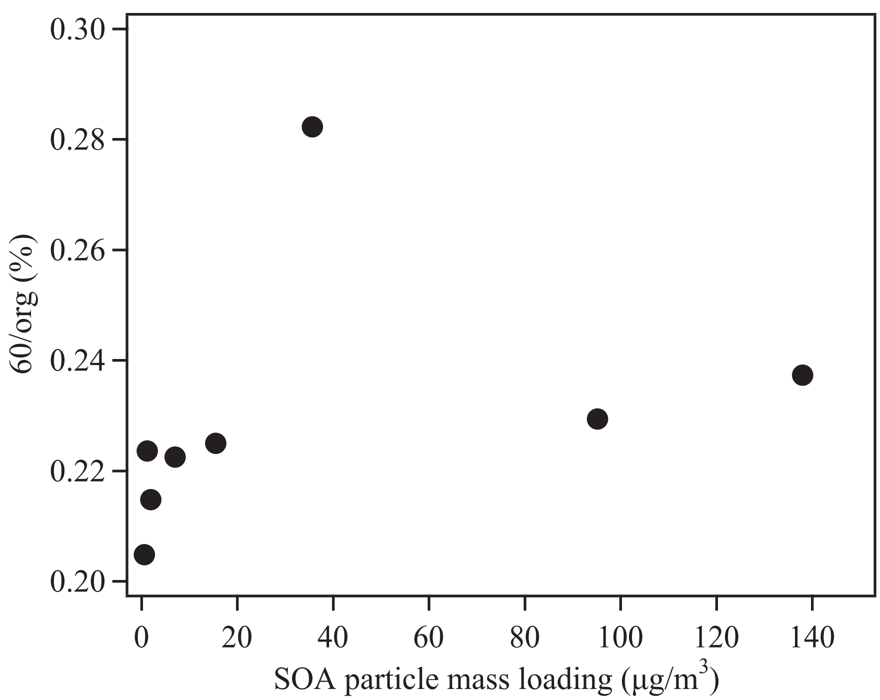
0.30
0.28
0.26
0.24
0.22
0.20
60/org (%)
0
20
40
60
80
100
120
140
SOA particle mass loading (µg/m3)

Figure S4